(Ga,Mn)As under pressure: A first-principles investigation

N. Gonzalez Szwacki,[1,*] Jacek A. Majewski,[1] and T. Dietl[1,2,3]

[1]*Institute of Theoretical Physics, Faculty of Physics, University of Warsaw, ul. Pasteura 5, PL-02-093 Warszawa, Poland*

[2]*Institute of Physics, Polish Academy of Sciences, al. Lotników 32/46, PL-02-668 Warszawa, Poland*

[3]*WPI-Advanced Institute for Materials Research (WPI-AIMR), Tohoku University, 2-1-1 Katahira, Aoba-ku, Sendai 980-8577, Japan*

(Received 24 February 2015; revised manuscript received 27 April 2015; published 18 May 2015)

Electronic and magnetic properties of $Ga_{1-x}Mn_xAs$, obtained from first-principles calculations employing the hybrid HSE06 functional, are presented for $x = 6.25\%$ and 12.5% under pressures ranging from 0 to 15 GPa. In agreement with photoemission experiments at ambient pressure, we find for $x = 6.25\%$ that nonhybridized Mn $3d$ levels and Mn-induced states reside about 5 and 0.4 eV below the Fermi energy, respectively. For elevated pressures, the Mn $3d$ levels, Mn-induced states, and the Fermi level shift toward higher energies, however the position of the Mn-induced states relative to the Fermi energy remains constant due to hybridization of the Mn $3d$ levels with the valence As $4p$ orbitals. We also evaluate, employing Monte Carlo simulations, the Curie temperature (T_C). At zero pressure, we obtain $T_C = 181$ K, whereas the pressure-induced changes in T_C are $dT_C/dp = +4.3$ K/GPa for $x = 12.5\%$ and an estimated value of $dT_C/dp \approx +2.2$ K/GPa for $x = 6.25\%$ under pressures up to 6 GPa. The determined values of dT_C/dp compare favorably with $dT_C/dp = +(2–3)$ K/GPa at $p \leqslant 1.2$ GPa found experimentally and estimated within the p-d Zener model for $Ga_{0.93}Mn_{0.07}As$ in the regime where hole localization effects are of minor importance [M. Gryglas-Borysiewicz *et al.*, Phys. Rev. B **82**, 153204 (2010)].

DOI: 10.1103/PhysRevB.91.184409 PACS number(s): 75.50.Pp, 75.30.Et, 78.20.Ls, 31.15.A−

I. INTRODUCTION

The application of hydrostatic pressure serves as a unique tool for tuning the various essential parameters in semiconductors [1]. High-pressure experiments and theoretical studies were important, for instance, in the delineation of the band structure of key semiconductors such as Si, Ge, and the III-V compounds [2]. This approach was also broadly used (both in theory and experiment) in studies of the bistability of donors (*DX* centers) in GaAs and GaN [3].

For spintronic semiconductors, high-pressure measurements can play an important role in understanding the mechanisms that are responsible for the coupling between magnetic ions in diluted magnetic semiconductors (DMSs): the changes in volume of the solid influence the local exchange interaction between magnetic dopants providing information about the mechanism responsible for the observed macroscopic magnetization [4]. Pressure can also help to elucidate the relationship between the coupling mechanism between magnetic dopants and the underlying band structure of the DMS. The states introduced by the dopants may have characteristics of the band-edge states and follow the band edge directly when the pressure is applied, or they may tend to be highly localized and therefore influenced by the entire Brillouin zone (the pressure dependence of deep levels does not follow any particular band edge) [5]. Bearing in mind the sensitivity of the exchange interaction between magnetic dopants to interatomic distances in DMSs, their experimental and *ab initio* theoretical studies under applied pressures are the most direct way to test different theoretical models that have been proposed to explain, for instance, the ferromagnetism in (Ga,Mn)As [6].

There exist a number of experimental studies on the variation of T_C under pressure for DMSs: (Pb,Sn,Mn)Te [7], (In,Mn)Sb [4,8], $(Sb,V)_2Te_3$ [9], (Ga,Mn)As [8,10], and (Ge,Mn)Te [11]. The results of those studies reveal that for samples with high concentrations of band holes, T_C increases with an increasing hydrostatic pressure p according to the expectations of the p-d Zener model [12]. However, there are two worthwhile exceptions, i.e., the systems showing $dT_C/dp < 0$. The first is a narrow-gap topological insulator $(Sb,V)_2Te_3$ [9], in which rather than intraband excitations (i.e., the standard Ruderman-Kittel-Kasuya-Yosida mechanism), interband excitations (i.e., the Bloembergen-Rowland interactions) give a dominant contribution to the coupling between localized spins of transition metals (TMs) [6]. The second is (Ga,Mn)As in the vicinity of the metal-insulator transition, where the increase in the p-d hybridization enhances hole localization and, hence, diminishes T_C [10].

Not much has been accomplished from the *ab initio* side so far. The pressure dependence of T_C for $Ga_{0.95}Mn_{0.05}As$ was studied by Bergqvist *et al.* [13] within the local-density approximation (LDA) and the LDA+U approach for pressures slightly crossing 7 GPa for which the direct-to-indirect band-gap transition occurs for GaAs within the LDA [14]. It was established (employing the LDA+U) that T_C increases for the decreasing lattice constant of $Ga_{0.95}Mn_{0.05}As$. This behavior was more pronounced within the mean-field approximation (MFA) than for the Monte Carlo (MC) simulations.

Here, we present first-principles calculations for the structural, electronic, and magnetic properties of $Mn_xGa_{1-x}As$ with $x = 6.25\%$ and 12.5%, exposed to pressures from 0 to 15 GPa. Therefore, we cover the whole range of pressures for which the zinc-blende structure of GaAs is stable [15]. Although the focus of this paper is to study the pressure dependence of T_C, some other issues are also discussed, such as the influence of pressure on the electronic and magnetic properties of $Ga_{0.9375}Mn_{0.0625}As$, the energetics of the formation of Mn pairs in GaAs, and finally the pressure dependence of the exchange coupling between Mn ions both at purely substitutional and mixed substitutional-interstitial sites.

*gonz@fuw.edu.pl

The paper is organized as follows. In Sec. II the computational approach is discussed. In Sec. III the results are presented, beginning with a discussion in Sec. III A of the structural, magnetic, and electronic properties of the studied DMS under pressure. The results concerning the cluster formation and the pressure dependence of T_C are presented in Secs. III B and III C, respectively. We end with some concluding remarks in Sec. IV.

II. COMPUTATIONAL DETAILS

The first-principles spin-polarized calculations are performed using a plane-wave basis and Troullier-Martins norm-conserving pseudopotentials [16,17] as implemented in the QUANTUM-ESPRESSO package [18]. We employ the hybrid HSE06 exchange-correlation functional [19,20] that appears to be particularly suitable for systems containing highly correlated localized electrons on TM d shells and itinerant band carriers [21,22], and in some cases outperforms any other functional [23,24]. The plane-wave cutoff is set to be 40 Ry, and a $8 \times 8 \times 8$ k-point mesh for the Brillouin zone sampling is used. The calculations are done using a body-centered-cubic lattice of supercells containing 32 atoms. Its primitive vectors are $\vec{a}_1 = a\,(-1,1,1)$, $\vec{a}_2 = a\,(1,-1,1)$, and $\vec{a}_3 = a\,(1,1,-1)$, where a is the edge of the conventional unit cell. By replacing one Ga ion with a Mn ion, we obtain a ferromagnetic (FM) DMS with the Mn concentration of 6.25%. We also study a system with two Mn ions in the Ga sublattice (it corresponds to Mn concentration of 12.5%). Finally, for completeness, we study a system with one substitutional and one interstitial Mn ion in a chosen supercell. The calculated equilibrium values of lattice constant, bulk modulus, and pressure derivative of the bulk modulus for GaAs are $a = 5.70$ Å, $B = 69.5$ GPa, and $B' = 4$, respectively, and they agree well with earlier theoretical and experimental reports [25,26]. Moreover, the computed GaAs lattice constant is close to the experimental values, 5.68 Å (5.70 Å) for $Ga_{1-x}Mn_xAs$ with $x \approx 6\%$ ($x \approx 12\%$) [27]. The Murnaghan equation of state is used to estimate the theoretical pressures. Since HSE06 calculations are computationally very demanding in comparison to PBE ones, the internal coordinates of atoms of GaAs doped with Mn were optimized at the PBE level of theory.

Structural optimization is a prerequisite to a successful computation of the electronic structure. This is because relaxation around the Mn impurity could, in principle, influence the electronic structure substantially. We have explicitly allowed for structural relaxation by displacing each atom from its equilibrium position for unit cells at zero and higher pressures. We find, for instance, that at zero pressure, the introduction of one Mn ion has a large effect on the position of the first shell of As neighbors, where the Mn-As bond length is elongated by 3.5% with respect to the Ga-As bond length of 2.469 Å in GaAs. The tetrahedral symmetry is preserved at all pressures.

The MC simulations are performed using the VAMPIRE software package [28]. The values of T_C are calculated from the thermal average of magnetization versus temperature curve. For these calculations, the cubic cell size is chosen to be $15a \times 15a \times 15a$, and for each temperature, we perform 240 000 equilibration steps and the averaging loop is set to 240 000 steps, which gives reasonable averaging.

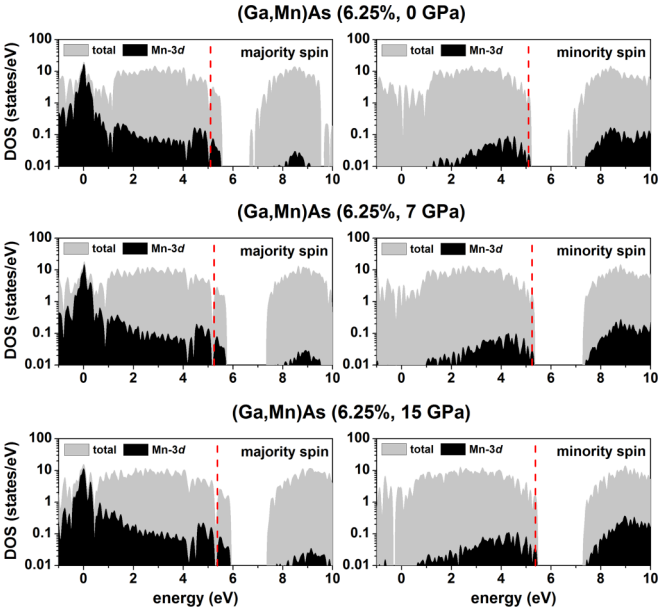

FIG. 1. (Color online) Spin-resolved DOS in logarithmic scale of $Mn_{0.0625}Ga_{0.9375}As$ (one Mn atom per supercell) at hydrostatic pressures of 0, 7, and 15 GPa. Light gray denotes the total DOS, whereas the Mn $3d$ projected DOS is shown in black. All the energy values are referred to the position of the main peak of the Mn $3d$ states. The dashed vertical line indicates the Fermi level.

III. RESULTS AND DISCUSSION

A. Structural, magnetic, and electronic properties

For $Ga_{1-x}Mn_x$ As with $x = 6.25\%$ and zero external pressure, we find a total magnetic moment of 4.27 Bohr magnetons (μ_B) per supercell. This value is reduced compared to the magnetic moment of $5\mu_B$ for the free Mn atom by spins of band holes that are aligned according to the antiferromagnetic p-d exchange interaction. We note that the orbital contribution to the magnetic moment, brought about by the spin-orbit interaction, is below $0.1\mu_B$ per Mn ion in (Ga,Mn) As [29,30]. For larger pressures, the total magnetic moment does not change significantly; for instance, for 7 and 15 GPa, it assumes the values of 4.23 and $4.19\mu_B$, respectively.

Calculations of the density of states are presented for hydrostatic pressures of 0, 7, and 15 GPa in Fig. 1. As seen, the majority and minority spin components show a band gap, indicating that the introduction of the Mn ions does not destroy the semiconducting nature of the material. This is further shown in Fig. 2, where we plot the pressure dependence of the majority spin band gap compared with that of pure GaAs. In the isolated impurity limit, Mn in GaAs is a shallow acceptor, situated ~0.1 eV above the valence-band maximum [31]. It hybridizes primarily with the valence band, and completely merges with it for a few percent of Mn (no impurity band). From Fig. 1, it is apparent that the introduction of Mn to GaAs results in the Mn-induced spin-splitting of the valence band, where the valence-band maximum of the majority spin is ~0.3 eV above that of the minority spin. This prediction is in qualitative but not quantitative agreement with experiment [32], since experimentally a smaller splitting of ~0.2 eV is expected for $x \approx 6\%$ [6]. It is, however, documented

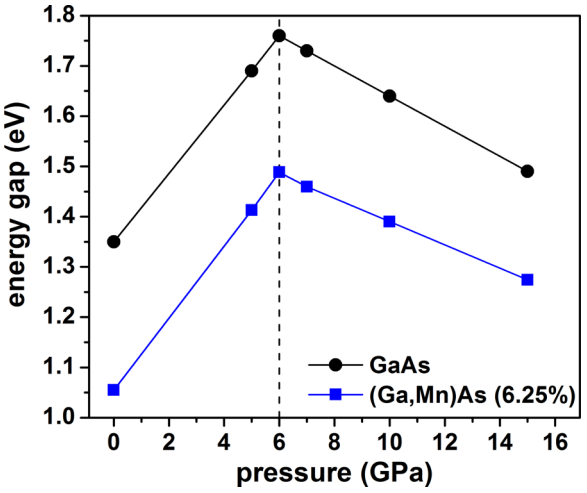

FIG. 2. (Color online) Majority spin band gap of $Ga_{0.9375}Mn_{0.0625}As$ and the band gap of GaAs plotted as a function of pressure. In both cases, the direct-to-indirect band-gap transition occurs at ∼6 GPa.

in the literature that the existing implementations of the density functional theory (DFT) tend to overestimate the *p*-*d* exchange splitting [33].

From Fig. 1, we can also see that the Fermi level is not located entirely within the majority band. This means that the system is not completely half-metallic, and as a consequence, the total magnetic moment per Mn ion is larger than $4\mu_B$. However, since our approach overestimates the exchange splitting, the real magnetic moment is closer to $5\mu_B$ than our theory predicts. The Mn 3*d* states in Fig. 1 are for zero pressure located 5.1 eV below the Fermi level. This value is slightly overestimated with respect to recent experimental results in which the main peak of the Mn 3*d* states was observed at 4.5 eV below the Fermi level [34]. However, it should be noted that the theoretical results for the location of the Mn 3*d* states depend strongly on the employed theoretical approach. The present results significantly improve previous DFT calculations that used the standard LDA or the generalized gradient approximation (GGA) [35]. In addition to the Mn 3*d* states, we also find, in agreement with experiment [34], Mn-induced states centered about 0.4 eV below the Fermi energy. For elevated pressures (7 and 15 GPa in Fig. 1), we obtain a pressure-induced shift of the Mn 3*d* levels, Mn-induced states, and the Fermi energy toward higher energies, whereas the position of the Mn-induced states relative to the Fermi energy remains constant. This is an additional indication for hybridization of the Mn 3*d* levels with the valence As 4*p* orbitals. It is also clear from our computations that the Mn-derived spin-polarized feature in the majority spin band gap is not detached from the host valence band (cf. Refs. [36,37]), and its pressure behavior is similar to that of the top of the valence band of the host material.

Finally, in Fig. 2 we plot the pressure dependence of the majority spin band gap for GaAs and $Ga_{0.9375}Mn_{0.0625}As$. GaAs has a direct band gap at ambient conditions. Under hydrostatic pressure, the upward shift of the conduction-band minimum at the Γ point eventually intersects the *X* minimum, and the material undergoes a direct-to-indirect band-gap transition observed experimentally at ∼4 GPa [38]. In Fig. 2, we can see that the pressure behavior of the band gap of $Ga_{0.9375}Mn_{0.0625}As$ is very similar to that of pure GaAs with a direct-to-indirect band-gap transition at ∼6 GPa.

TABLE I. Dissociation energies, interionic distances, and total energy differences per ion between FM and AFM states for various configurations of Mn complexes in GaAs at zero pressure. Results for an isolated Mn dimer (Mn_2) are also included.

	Dissociation energy (eV)	d (Å)	$E_{FM} - E_{AFM}$ (meV/Mn)
Mn_S-$Mn_{I(Ga)}$	0.42	2.699	69
Mn_S-$Mn_{I(As)}$	0.18	2.879	33
Mn_2	0.21	3.243	30
Mn_S-Mn_S	0.11	3.994	− 39

B. Cluster formation

We consider the case of the formation of clusters composed of two Mn ions in GaAs. It is well established [39–42] that the magnetic ions may occupy both substitutional cation sites, Mn_S, and As- and Ga-coordinated tetrahedral interstitial sites, $Mn_{I(As)}$ and $Mn_{I(Ga)}$, respectively.

We start first with the configuration where the interstitial and substitutional ions are as far away from each other as possible within the supercell. For this case, we obtain that (Mn_S,$Mn_{I(Ga)}$) is more stable than (Mn_S,$Mn_{I(As)}$) by 0.11 eV. This result is congruent with previous computations [39–42].

Let us now focus on the formation of Mn_S-Mn_S and Mn_S-Mn_I complexes in GaAs. In both types of considered clusters, the Mn ions are the nearest neighbors (NNs). The dissociation energies for Mn_S-Mn_S, Mn_S-$Mn_{I(As)}$, and Mn_S-$Mn_{I(Ga)}$ pairs are defined as

$$\begin{aligned} \Delta E_{SS} &= E(Mn_S,Mn_S) - E(Mn_S\text{-}Mn_S), \\ \Delta E_{SI(As)} &= E(Mn_S,Mn_{I(Ga)}) - E(Mn_S\text{-}Mn_{I(As)}), \\ \Delta E_{SI(Ga)} &= E(Mn_S,Mn_{I(Ga)}) - E(Mn_S\text{-}Mn_{I(Ga)}), \end{aligned} \quad (1)$$

respectively, where E is the total energy of the 32- or 33-atom supercell. To calculate $E(Mn_S,Mn_S)$ and $E(Mn_S,Mn_{I(Ga)})$, we place the magnetic ions as far away from each other as possible within the supercell. The largest possible distance between the magnetic ions is 5.701 and 6.179 Å for (Mn_S,Mn_S) and (Mn_S,$Mn_{I(Ga)}$), respectively. The calculated dissociation energies are 0.11, 0.18, and 0.42 eV for ΔE_{SS}, $\Delta E_{SI(As)}$, and $\Delta E_{SI(Ga)}$, respectively. Our results suggest that pairs involving Mn_I are more likely to be present than purely substitutional clusters. It should also be noted that clusters involving Ga-coordinated interstitials are more stable than those involving As-coordinated interstitials. All mentioned values and some additional details for the Mn complexes in GaAs are summarized in Table I, where for comparison, we also include the isolated Mn_2 dimer for which we predict an antiferromagnetic (AFM) coupling with a binding energy of 0.21 eV, in agreement with more sophisticated calculations involving quantum-chemical methods [43]. The activation energy for the outdiffusion of charged Mn_I ions that are bound in interstitial-substitutional complexes is a sum of the dissociation energy plus the energy barrier for diffusion of

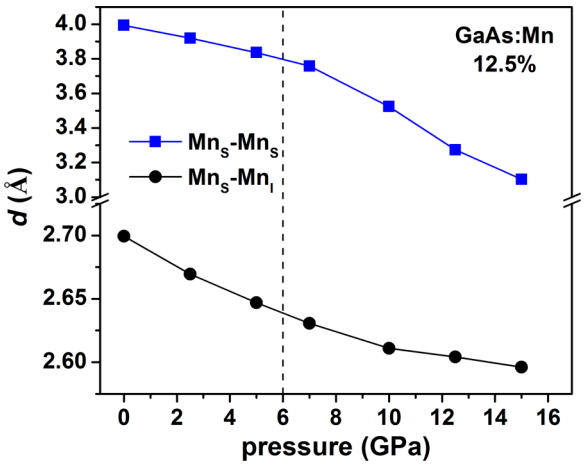

FIG. 3. (Color online) Nearest-neighbor distances d plotted as a function of pressure for Mn_S-$Mn_{I(Ga)}$ (circles) and Mn_S-Mn_S (squares) pairs in GaAs.

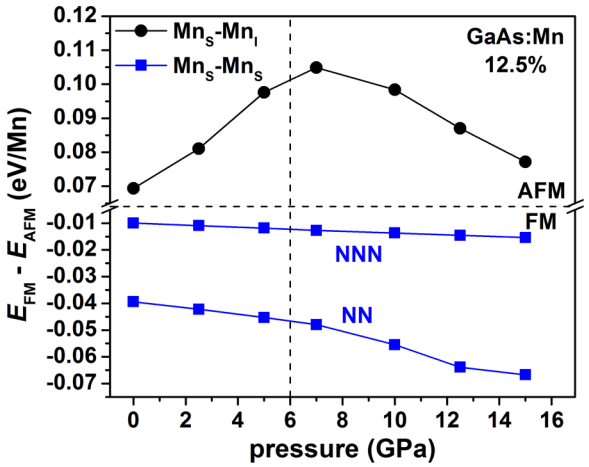

FIG. 4. (Color online) Total energy difference per ion between the FM and AFM configurations for Mn_S-$Mn_{I(Ga)}$ (circles) and Mn_S-Mn_S (squares) pairs in GaAs as a function of pressure. For Mn_S-Mn_S, we have considered NN and NNN positions in the Ga sublattice.

charged Mn_I ions between interstitial sites [40,42]. It should be noted, however, that the computed by us dissociation energies for clusters involving neutral Mn_I ions are equal to activation energies because of the lack of the migration barrier for swapping of neutral Mn_I ions between interstitial sites [42].

Finally, in Fig. 3, we show the Mn-Mn NN distance d as a function of pressure. It is clear from the figure that the variation with pressure of $d(Mn_S\text{-}Mn_{I(Ga)})$ is much smaller than that of $d(Mn_S\text{-}Mn_S)$. For comparison, at zero pressure the unrelaxed values of $d(Mn_S\text{-}Mn_S)$ and $d(Mn_S\text{-}Mn_{I(Ga)})$—where atoms are placed into ideal lattice positions—are 4.032 and 2.469 Å, respectively (the relaxed values are listed in Table I).

C. Curie temperature

It is well established [6] that one of the factors limiting high-temperature ferromagnetism is the presence of Mn_S-Mn_I complexes in GaAs in which the Mn ions exhibit an AFM coupling. This coupling is not only preserved but tends to increase in strength with pressure (for pressures up to ~7 GPa). This is shown in Fig. 4, where we plotted the total energy difference, $E_{FM} - E_{AFM}$, between the FM and AFM configurations for Mn_S-$Mn_{I(Ga)}$ and Mn_S-Mn_S pairs as a function of pressure. For the substitutional Mn ions, we have considered NN and next-nearest-neighbor (NNN) positions in the Ga sublattice.

The energy difference $E_{FM} - E_{AFM}$ for the substitutional ions can be used to evaluate the exchange interaction J_{ij} between i- and j-site local spins. The exchange energy for a system of interacting atomic moments is given by the effective classical Heisenberg Hamiltonian $H = -\sum_{i\neq j} J_{ij}\vec{S}_i\vec{S}_j = -2\sum_{i<j} J_{ij}\vec{S}_i\vec{S}_j$, where in our case $S_i = S_j = S = 5/2$. For ferromagnetically coupled Mn ions at NN substitutional positions, $-2J_{NN}S^2 = E_{FM} - E_{AFM}$. For zero pressure, $E_{FM} - E_{AFM} = -39$ meV/Mn, therefore we obtain that $J_{NN}S^2 = 20$ meV; the calculated in a similar way $J_{NNN}S^2$ for NNNs gives a modest value of 5 meV [44]. The Curie temperature in the MFA is given by

$$T_C = (2/3k_B)\left(x\sum_j z_j J_{0j} S^2\right)$$
$$= (2S^2/3k_B)(12J_{NN} + 6J_{NNN})/8, \quad (2)$$

where x is the concentration of Mn and z_j denotes the number of sites on the jth shell. The Curie temperature versus pressure is plotted in Fig. 5. From the slope of the MFA curve, we can estimate the derivative of temperature with respect to pressure, $dT_C/dp = 7$ K/GPa, for pressures close to zero. A linear dependence of the MFA curve extends, however, up to ~6 GPa. Assuming a linear dependence of the Curie temperature versus manganese concentration, we can estimate that for a 6.25% concentration of Mn, $dT_C/dp = 3.5$ K/GPa. Beyond 6 GPa,

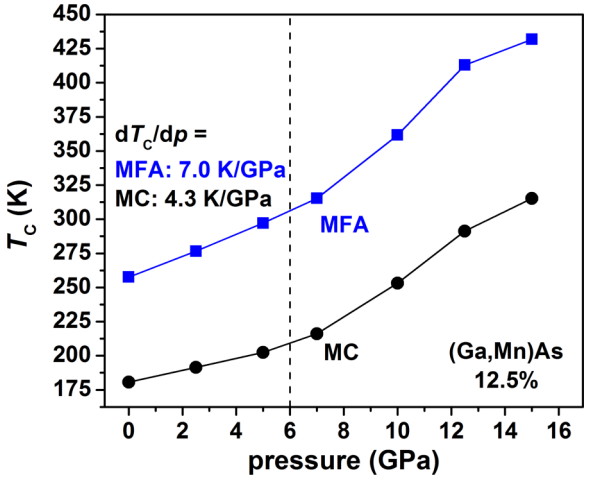

FIG. 5. (Color online) Curie temperature of (Ga,Mn)As calculated within MFA (squares) and MC (circles) methods as a function of pressure. The given values of the pressure coefficients correspond to the region below 6 GPa marked by a dashed line.

the Curie temperature increases even faster, reaching room temperature for ∼7 GPa.

We have also carried out MC simulations using the same exchange parameters J_{NN} and J_{NNN} as determined above. From Fig. 5, we can see that the pressure behavior of T_C calculated by means of MC is similar to that obtained from MFA calculations. However, the critical temperature is shifted down, for all pressures, by an average value of 26%. For pressures close to 0 GPa, $dT_C/dp = 4.3$ K/GPa, and an estimated value for $x = 6.25\%$ would be $dT_C/dp = 2.2$ K/GPa, which is in the range of values obtained experimentally, $dT_C/dp = (2–3)$ K/GPa at $p \leqslant 1.2$ GPa, and estimated within the p-d Zener model for $Ga_{0.93}Mn_{0.07}As$ [10].

IV. CONCLUSIONS

In this paper, we have presented the pressure dependence of the Curie temperature for $Ga_{1-x}Mn_xAs$ with experimentally realistic Mn contents of $x = 6.25\%$ and 12.5%, using the hybrid HSE06 functional for the description of exchange and correlation effects. In agreement with photoemission experiments, we have found for $x = 6.25\%$ and ambient pressure that the nonhybridized Mn $3d$ levels and Mn-induced states reside about 5 and 0.4 eV below the Fermi energy, respectively. For elevated pressures, the Mn $3d$ levels, Mn-induced states, and the Fermi level shift toward higher energies, however the position of the Mn-induced states relative to the Fermi energy remains constant due to hybridization of the Mn $3d$ levels with the valence As $4p$ orbitals. It follows from our computations that the Mn-derived spin-polarized feature in the majority spin band gap is not detached from the host valence band, and its pressure behavior is similar to that of the top of the valence band of the host material. We have also found that T_C at zero pressure is 181 and 258 K for MC and MFA calculations for $x = 12.5\%$, respectively, while it increases linearly under pressures up to 6 GPa. The pressure-induced changes in T_C estimated for $x = 6.25\%$ are +2.2 and +3.5 K/GPa for MC and MFA calculations, respectively. The determined values of dT_C/dp compare well with those found experimentally and estimated within the p-d Zener model for $Ga_{0.93}Mn_{0.07}As$ in the regime in which hole localization effects are of lesser importance [10].

ACKNOWLEDGMENTS

The work was supported by the European Research Council through the FunDMS Advanced Grant within the "Ideas" Seventh Framework Programme of the EC and Narodowe Centrum Nauki in Poland (Decision No. 2011/02/A/ST3/00125). We acknowledge the access to the computing facilities of the Interdisciplinary Center of Modeling at the University of Warsaw.

[1] P. Y. Yu, High pressure semiconductor physics: Looking toward the future on the shoulder of the past, Phys. Status Solidi B **248**, 1077 (2011).

[2] E. Ghahramani and J. E. Sipe, Pressure dependence of the band gaps of semiconductors, Phys. Rev. B **40**, 12516 (1989).

[3] C. G. Van de Walle, and J. Neugebauer, First-principles calculations for defects and impurities: Applications to III-nitrides, J. Appl. Phys. **95**, 3851 (2004).

[4] M. Csontos, G. Mihaly, B. Janko, T. Wojtowicz, X. Liu, and J. K. Furdyna, Pressure-induced ferromagnetism in (In,Mn)Sb dilute magnetic semiconductor, Nat. Mater. **4**, 447 (2005).

[5] R. Willardson, E. Weber, W. Paul, and T. Suski, *High Pressure Semiconductor Physics I* (Elsevier Science, Amsterdam, 1998).

[6] T. Dietl and H. Ohno, Dilute ferromagnetic semiconductors: Physics and spintronic structures, Rev. Mod. Phys. **86**, 187 (2014).

[7] T. Suski, J. Igalson, and T. Story, Ferromagnetism of (Pb,Sn,Mn)Te under high pressure, J. Magn. Magn. Mater. **66**, 325 (1987).

[8] M. Csontos, G. Mihály, B. Janko, T. Wojtowicz, W. L. Lim, X. Liu, and J. K. Furdyna, Effect of hydrostatic pressure on the transport properties in magnetic semiconductors, Phys. Status Solidi C **1**, 3571 (2004).

[9] J. S. Dyck, T. J. Mitchell, A. J. Luciana, P. C. Quayle, v. Drašar, and P. Lošťák, Significant suppression of ferromagnetism by hydrostatic pressure in the diluted magnetic semiconductor $Sb_{2-x}V_xTe_3$ with $x \leqslant 0.03$, Appl. Phys. Lett. **91**, 122506 (2007).

[10] M. Gryglas-Borysiewicz, A. Kwiatkowski, M. Baj, D. Wasik, J. Przybytek, and J. Sadowski, Hydrostatic pressure study of the paramagnetic-ferromagnetic phase transition in (Ga,Mn)As, Phys. Rev. B **82**, 153204 (2010).

[11] S. T. Lim, J. F. Bi, L. Hui, and K. L. Teo, Exchange interaction and Curie temperature in $Ge_{1-x}Mn_xTe$ ferromagnetic semiconductors, J. Appl. Phys. **110**, 023905 (2011).

[12] T. Dietl, H. Ohno, F. Matsukura, J. Cibert, and D. Ferrand, Zener model description of ferromagnetism in zinc-blende magnetic semiconductors, Science **287**, 1019 (2000).

[13] L. Bergqvist, B. Belhadji, S. Picozzi, and P. H. Dederichs, Volume dependence of the Curie temperatures in diluted magnetic semiconductors, Phys. Rev. B **77**, 014418 (2008).

[14] J. Sjakste, V. Tyuterev, and N. Vast, *Ab initio* study of Γ-X intervalley scattering in GaAs under pressure, Phys. Rev. B **74**, 235216 (2006).

[15] S. T. Weir, Y. K. Vohra, C. A. Vanderborgh, and A. L. Ruoff, Structural phase transitions in GaAs to 108 GPa, Phys. Rev. B **39**, 1280 (1989).

[16] We use the pseudopotentials As.pbe-mt_fhi.UPF, Ga.pbe-mt_fhi.UPF, and Mn.pbe-mt_fhi.UPF from http://www.quantum-espresso.org.

[17] N. Troullier and J. L. Martins, Efficient pseudopotentials for plane-wave calculations, Phys. Rev. B **43**, 1993 (1991).

[18] G. Paolo, B. Stefano, B. Nicola, C. Matteo, C. Roberto, C. Carlo, C. Davide, L. C. Guido, C. Matteo, D. Ismaila, C. Andrea Dal, G. de Stefano, F. Stefano, F. Guido, G. Ralph, G. Uwe, G. Christos, K. Anton, L. Michele, M.-S. Layla, M. Nicola, M. Francesco, M. Riccardo, P. Stefano, P. Alfredo, P. Lorenzo, S. Carlo, S. Sandro, S. Gabriele, P. S. Ari, S. Alexander, U. Paolo, and M. W. Renata, Quantum espresso: A modular and open-source software project for quantum simulations of materials, J. Phys.: Condens. Matter **21**, 395502 (2009).

[19] J. Heyd, G. E. Scuseria, and M. Ernzerhof, Hybrid functionals based on a screened Coulomb potential, J. Chem. Phys. **118**, 8207 (2003).

[20] J. Heyd, G. E. Scuseria, and M. Ernzerhof, Erratum: Hybrid functionals based on a screened Coulomb potential; J. Chem. Phys. **118**, 8207 (2003); **124**, 219906 (2006).

[21] A. Stroppa and G. Kresse, Unraveling the Jahn-Teller effect in Mn-doped GaN using the Heyd-Scuseria-Ernzerhof hybrid functional, Phys. Rev. B **79**, 201201 (2009).

[22] A. Stroppa, G. Kresse, and A. Continenza, Revisiting Mn-doped Ge using the Heyd-Scuseria-Ernzerhof hybrid functional, Phys. Rev. B **83**, 085201 (2011).

[23] C. Freysoldt, B. Grabowski, T. Hickel, J. Neugebauer, G. Kresse, A. Janotti, and C. G. Van de Walle, First-principles calculations for point defects in solids, Rev. Mod. Phys. **86**, 253 (2014).

[24] S. Kümmel and L. Kronik, Orbital-dependent density functionals: Theory and applications, Rev. Mod. Phys. **80**, 3 (2008).

[25] R. Peverati and D. G. Truhlar, Performance of the M11-L density functional for bandgaps and lattice constants of unary and binary semiconductors, J. Chem. Phys. **136**, 134704 (2012).

[26] M. Schlipf, M. Betzinger, C. Friedrich, M. Ležaić, and S. Blügel, HSE hybrid functional within the FLAPW method and its application to GdN, Phys. Rev. B **84**, 125142 (2011).

[27] H. Ohno, A. Shen, F. Matsukura, A. Oiwa, A. Endo, S. Katsumoto, and Y. Iye, (Ga,Mn)As: A new diluted magnetic semiconductor based on GaAs, Appl. Phys. Lett. **69**, 363 (1996).

[28] R. F. L. Evans, W. J. Fan, P. Chureemart, T. A. Ostler, M. O. A. Ellis, and R. W. Chantrell, Atomistic spin model simulations of magnetic nanomaterials, J. Phys.: Condens. Matter **26**, 103202 (2014).

[29] P. Wadley, A. A. Freeman, K. W. Edmonds, G. van der Laan, J. S. Chauhan, R. P. Campion, A. W. Rushforth, B. L. Gallagher, C. T. Foxon, F. Wilhelm, A. G. Smekhova, and A. Rogalev, Element-resolved orbital polarization in (III,Mn)As ferromagnetic semiconductors from K-edge x-ray magnetic circular dichroism, Phys. Rev. B **81**, 235208 (2010).

[30] C. Śliwa and T. Dietl, Orbital magnetization in dilute ferromagnetic semiconductors, Phys. Rev. B **90**, 045202 (2014).

[31] M. Linnarsson, E. Janzén, B. Monemar, M. Kleverman, and A. Thilderkvist, Electronic structure of the GaAs:Mn_{Ga} center, Phys. Rev. B **55**, 6938 (1997).

[32] J. Szczytko, W. Mac, A. Twardowski, F. Matsukura, and H. Ohno, Antiferromagnetic p-d exchange in ferromagnetic $Ga_{1-x}Mn_xAs$ epilayers, Phys. Rev. B **59**, 12935 (1999).

[33] S.-H. Wei and A. Zunger, Electronic origins of the magnetic phase transitions in zinc-blende Mn chalcogenides, Phys. Rev. B **48**, 6111 (1993).

[34] A. X. Gray, J. Minár, S. Ueda, P. R. Stone, Y. Yamashita, J. Fujii, J. Braun, L. Plucinski, C. M. Schneider, G. Panaccione, H. Ebert, O. D. Dubon, K. Kobayashi, and C. S. Fadley, Bulk electronic structure of the dilute magnetic semiconductor $Ga_{1-x}Mn_xAs$ through hard X-ray angle-resolved photoemission, Nat. Mater. **11**, 957 (2012).

[35] R. R. Pela, M. Marques, L. G. Ferreira, J. Furthmuller, and L. K. Teles, GaMnAs: Position of Mn-d levels and majority spin band gap predicted from GGA-1/2 calculations, Appl. Phys. Lett. **100**, 202408 (2012).

[36] I. Di Marco, P. Thunström, M. I. Katsnelson, J. Sadowski, K. Karlsson, S. Lebègue, J. Kanski, and O. Eriksson, Electron correlations in $Mn_xGa_{1-x}As$ as seen by resonant electron spectroscopy and dynamical mean field theory, Nat. Commun. **4**, 2645 (2013).

[37] J. Fujii, B. R. Salles, M. Sperl, S. Ueda, M. Kobata, K. Kobayashi, Y. Yamashita, P. Torelli, M. Utz, C. S. Fadley, A. X. Gray, J. Braun, H. Ebert, I. Di Marco, O. Eriksson, P. Thunström, G. H. Fecher, H. Stryhanyuk, E. Ikenaga, J. Minár, C. H. Back, G. van der Laan, and G. Panaccione, Identifying the electronic character and role of the Mn states in the valence band of (Ga,Mn)As, Phys. Rev. Lett. **111**, 097201 (2013).

[38] P. Grivickas, M. D. McCluskey, and Y. M. Gupta, Transformation of GaAs into an indirect L-band-gap semiconductor under uniaxial strain, Phys. Rev. B **80**, 073201 (2009).

[39] J. Mašek and F. Máca, Interstitial Mn in (Ga,Mn)As: Binding energy and exchange coupling, Phys. Rev. B **69**, 165212 (2004).

[40] K. W. Edmonds, P. Bogusławski, K. Y. Wang, R. P. Campion, S. N. Novikov, N. R. S. Farley, B. L. Gallagher, C. T. Foxon, M. Sawicki, T. Dietl, M. Buongiorno Nardelli, and J. Bernholc, Mn interstitial diffusion in (Ga,Mn)As, Phys. Rev. Lett. **92**, 037201 (2004).

[41] P. Mahadevan and A. Zunger, Ferromagnetism in Mn-doped GaAs due to substitutional-interstitial complexes, Phys. Rev. B **68**, 075202 (2003).

[42] V. I. Baykov, P. A. Korzhavyi, and B. Johansson, Diffusion of interstitial Mn in the dilute magnetic semiconductor (Ga,Mn)As: The effect of a charge state, Phys. Rev. Lett. **101**, 177204 (2008).

[43] A. A. Buchachenko, G. Chałasiński, and M. M. Szczęśniak, Electronic structure and spin coupling of the manganese dimer: The state of the art of *ab initio* approach, J. Chem. Phys. **132**, 024312 (2010).

[44] In the 32-atom unit cell, each Mn ion has two NNN; therefore, in order to calculate the NNN exchange constant, we have divided $E_{FM} - E_{AFM}$ additionally by a factor of 2.